2015

Internal stresses in pre-stressed micron-scale aluminum core-shell particles and their improved reactivity

Valery I. Levitas
Iowa State University, vlevitas@iastate.edu

Jena McCollum
Texas Tech University

Michelle L. Pantoya
Texas Tech University

Nobumichi Tamura
Lawrence Berkeley National Laboratory

Internal stresses in pre-stressed micron-scale aluminum core-shell particles and their improved reactivity

Abstract

Dilatation of aluminum (Al) core for micron-scale particles covered by alumina (Al_2O_3) shell was measured utilizing x-ray diffraction with synchrotron radiation for untreated particles and particles after annealing at 573 K and fast quenching at 0.46 K/s. Such a treatment led to the increase in flame rate for Al + CuO composite by 32% and is consistent with theoretical predictions based on the melt-dispersion mechanism of reaction for Al particles. Experimental results confirmed theoretical estimates and proved that the improvement of Al reactivity is due to internal stresses. This opens new ways of controlling particle reactivity through creating and monitoring internal stresses.

Disciplines

Aerospace Engineering | Structures and Materials

Comments

This article is published as Levitas, Valery I., Jena McCollum, Michelle L. Pantoya, and Nobumichi Tamura. "Internal stresses in pre-stressed micron-scale aluminum core-shell particles and their improved reactivity." Journal of Applied Physics 118, no. 9 (2015): 094305. doi: 10.1063/1.4929642. Posted with permission.

Internal stresses in pre-stressed micron-scale aluminum core-shell particles and their improved reactivity

Valery I. Levitas, Jena McCollum, Michelle L. Pantoya, and Nobumichi Tamura

Citation: Journal of Applied Physics **118**, 094305 (2015);
View online: https://doi.org/10.1063/1.4929642
View Table of Contents: http://aip.scitation.org/toc/jap/118/9
Published by the American Institute of Physics

Internal stresses in pre-stressed micron-scale aluminum core-shell particles and their improved reactivity

Valery I. Levitas,[1,a)] Jena McCollum,[2] Michelle L. Pantoya,[2] and Nobumichi Tamura[3]
[1]*Department of Aerospace Engineering, Department of Mechanical Engineering, Department of Material Science and Engineering, Iowa State University, Ames, Iowa 50011, USA*
[2]*Mechanical Engineering, Texas Tech University, Lubbock, Texas 79409, USA*
[3]*Advanced Light Source, Lawrence Berkeley National Laboratory, Berkeley, California 94720, USA*

(Received 26 June 2015; accepted 16 August 2015; published online 3 September 2015)

Dilatation of aluminum (Al) core for micron-scale particles covered by alumina (Al_2O_3) shell was measured utilizing x-ray diffraction with synchrotron radiation for untreated particles and particles after annealing at 573 K and fast quenching at 0.46 K/s. Such a treatment led to the increase in flame rate for Al + CuO composite by 32% and is consistent with theoretical predictions based on the melt-dispersion mechanism of reaction for Al particles. Experimental results confirmed theoretical estimates and proved that the improvement of Al reactivity is due to internal stresses. This opens new ways of controlling particle reactivity through creating and monitoring internal stresses.
 [http://dx.doi.org/10.1063/1.4929642]

I. INTRODUCTION

Interest in reaction of aluminum (Al) particles with various oxidizers is based on the high energy density of Al and possibility to reach high reaction rates and flame speeds. Thus, Al nanoparticles with different oxidizers (e.g., MoO_3) produce flame speed ups to 1 km/s.[1–5] Such high reaction rates were explained by postulating a new mechanochemical reaction mechanism coined the melt-dispersion mechanism (MDM),[4,6–8] which for fast heating rates substitutes the traditional diffusion mechanism.[9–11] The key point of the MDM is that Al melting is accompanied by a 6% volumetric expansion strain, which generates pressures of 1 to 3 GPa in the molten Al core and tensile hoop stress σ_h in the Al oxide shell that exceeds 10 GPa and the ultimate strength of alumina. During fast heating and, consequently, loading, such stresses do not have time to relax and cause the dynamic fracture and spallation of the alumina shell. Spallation of the shell causes the pressure to approach zero at the bare Al surface, while pressure within the molten core does not initially change. This pressure imbalance produces an unloading spherical wave propagating to the center of the core, which generates a tensile pressure up to 8 GPa at the center in the reflected wave. Such a pressure wave significantly exceeds the cavitation limit of liquid Al and disperses the Al core into small bare fragments. Convective gas flow and multiple particle collisions facilitate this mechanism. Thus, MDM transforms a single Al particle covered by an Al_2O_3 shell into hundreds or thousands of smaller bare molten particles, and reaction is no longer limited by diffusion through the initial oxide shell.

In addition to some qualitative confirmations summarized in Ref. 8 (see also Ref. 12), one of the main quantitative confirmations of the MDM is related to reproduction of a sophisticated relationship between the relative flame propagation rate V/V_{max} and the relative particle size $M = R/\delta$.[4,6,8,13] Here, V is the flame propagation rate and V_{max} is the maximum possible flame propagation rate in the given experimental set-up under the same conditions (e.g., same initial bulk density of reactive mixture, oxidizer, stoichiometry, etc.); R is the radius of the Al core and δ is the shell thickness. Flame rate V_{max} is achieved for nanoparticles. This equation enabled predictions (e.g., that are exactly opposite to those based on the diffusion mechanism) and suggested methods to increase the flame propagation rate and particle reactivity. Since for large M, V/V_{max} tends to a finite value (i.e., 0.4–0.5 for Al), activation of the MDM and high flame rates were predicted and confirmed experimentally for 1–4.5 μm particles.[13,14] These studies suggest that micron-scale Al particles have the potential for demonstrating high reactivity in accordance with the MDM.

Another prediction is that creating initial compressive stress in the shell and tensile stress in the core would delay shell fracture during heating and increase V/V_{max}.[6] This prediction is based on the obtained relationship[6] that V/V_{max} is equal to the concentration of molten Al in Al core that causes fracture of the oxide shell. That means that only the part of the Al core that is molten at the instant of shell fracture is dispersed and participates in reaction while the flame front passes through. By producing initial compressive stresses in the shell, we strengthen the shell against fracture under action of internal pressure during Al core melting. That means that a higher concentration of melt is required to fracture the shell, which (due to obtained equality of melt concentration and V/V_{max}) increases V/V_{max}. Thus, MDM predicts increased reactivity of Al particles by increasing the temperature T_0 at which internal thermal stresses in the core-shell system are zero. Traditionally, T_0 coincides with the temperature at which the initial oxide shell is formed, i.e., in most cases room temperature. Heating and annealing Al nano- and micron-scale particles at higher temperature T_a lead to relaxation of internal stresses and changed T_0 to T_a.

a)Author to whom correspondence should be addressed. Electronic mail: vlevitas@iastate.edu

For the fast quench rate, these stresses may not have time to relax during cooling and T_0 remained T_a. Such change in T_0 to 378 K increased flame rate for $Al + MoO_3$ by 31% for nano-Al and by 41% for micron-Al particles,[15] both in quantitative agreements with theoretical predictions. Reference 16 was focused on micron scale particles and increase T_0 to four values in a range 383–473 K. The best treatment increased flame rate by 36% and reaches 68% of the flame rate of the best Al nanoparticles in the same set up. This has important practical implication, because micron particles are 30–50 times less expensive than nanoparticles and do not possess safety and environmental issues typical of nanoparticles.

However, in all previous works related to MDM, stresses were determined theoretically and have never been confirmed experimentally. Without strain measurements to confirm theoretical predictions, there is a possibility that observed improvement is caused by another hypothetical reason. If this would be the case, it also eliminates important confirmations of the MDM. The goal of the current paper is to measure stresses in Al experimentally before and after thermal treatment and compare results with theoretical predictions. Also, flame propagation rate will be measured for untreated and treated particles to be sure that the treatment indeed leads to increasing reactivity. We would like to mention some previous publication on the measurements of lattice parameters and stresses in Al particles,[11,17,18] but they were not related to change in T_0 due to annealing.

II. EXPERIMENTAL

Aluminum and copper oxide powders were combined to an equivalence ratio of 1.2. The aluminum (Al) powder has an average particle diameter of 5 μm, and the copper oxide (CuO) has an average particle diameter of 50 nm. Characterization of Al particles including size distribution and width of oxide shell was presented in Ref. 16. The powder mixtures were prepared for an equivalence ratio of 1.2, then loaded into 3 mm inner diameter and 10 cm long quartz tubes containing 550 mg of powder each, i.e., 16% of theoretical mass density (TMD). Both ends of the tube were sealed with one side securing a length of Nichrome wire for thermal ignition. The filled tubes were inserted into a vacuum oven, heated to 573 K at a rate of 10 KPM, and held at that temperature for 15 min. The temperature of the powder was monitored with a thermocouple. The tubes were then cooled to room temperature by placing the tube filled powder in a refrigerator. Temperature variation is described in Ref. 16. The averaged cooling rate is 0.46 KPS.

Each tube was placed inside a blast chamber for *ignition and flame propagation experiments*. The powders were ignited using a hot wire, and flame propagation was recorded with a Phantom v7 (Vision Research, Wayne, NJ) high speed camera at a rate of 63 000 frames per second and 512×128 resolution. The camera was aligned perpendicular to the direction of flame propagation. Flame speed was determined by tracking the flame front through a referenced time and distance using the Vision Research Software. The resolution of the flame speed for this diagnostic is 0.1 m/s. The largest source of uncertainty in the measurement is due to repeatability and is shown for each data set in the results.

X-Ray Diffraction experiments were performed at the Advanced Light Source on beamline 12.3.2 using a micron focused synchrotron x-ray beam. Small quantity of the aluminum particles was spread over glass slides and scanned under the x-ray beam (either polychromatic or monochromatic), while a diffraction pattern was collected at each step using a DECTRIS Pilatus 1 M detector. The measured relative small shifts in the reflection positions in the Laue pattern provide the deviatoric strain tensor of the material, while the measurement of the energy of one reflection provides the dilatational component. Data were processed using the XMAS software.[19] The beamline experimental setup and capabilities have been described elsewhere.[20] Note that time between heat treatment and x-ray diffraction was 46 days, during which internal stresses partially relaxed. Selected experiments after 19 days showed larger stresses but due to insufficient statistics they will not be presented here.

III. RESULTS

Flame speeds measured for the controlled, untreated powders are 220 ± 10 m/s. Once the samples are annealed to 573 K, they experience a 32% increase in flame speed measured at 291 ± 10 m/s. This is a significant increase in reactivity for the composite, qualitatively consistent with data in Ref. 16 for looser powder of 8% of TMD. However, quantitatively, an increase of flame speed by 36% was obtained in Ref. 16 after annealing at 473 K. This means that further increase of annealing temperature beyond 473 K does not improve reactivity. This may be related to the fact that at cooling from such a high temperature (i.e., 573 K) internal stresses have time to partially relax and are approximately at the same level as at annealing at 473 K. That is why we will use $T_0 = 473$ K in our estimates below. Also, the effect of larger TMD (e.g., 16% vs 8% TMD) may be partially responsible for reduced flame speed of treated and untreated particles.

X-ray diffraction analysis was performed for the samples. Fig. 1 shows the results of dilatation (i.e., volumetric) strain distribution measurements of aluminum particles that were (a) untreated and (b) annealed to 573 K. The aluminum particles annealed to 573 K and cooled to room temperature showed a significant dilatational strain increase from the baseline Al particles. An average over volume of all particles for dilatational strain is $\varepsilon_0 = 3.9 \times 10^{-6}$ for untreated particles and $\varepsilon_0 = 2.87 \times 10^{-5}$ for annealed particles. They produce the tensile mean stress $\sigma_0 = K_1 \varepsilon_0$, where $K_1 = 76$GPa (Ref. 21) is the bulk modulus of Al at 573 K, which is 0.296 MPa before treatment and 2.18 MPa after treatment. The maximum number of counts (i.e., the maximum volume of aluminum that exhibits such a volumetric strain) is in the range 0 to 2×10^{-5} for untreated particles (corresponding mean stress is 0 to 1.52 MPa) and 6 to 8×10^{-5} for annealed particles (corresponding mean stress is 4.56 to 6.08 MPa).

Figure 1 also contains the distribution of the average diffraction peak width in degrees for (c) untreated particles and (d) particles annealed to 573 K. The diffraction peak width

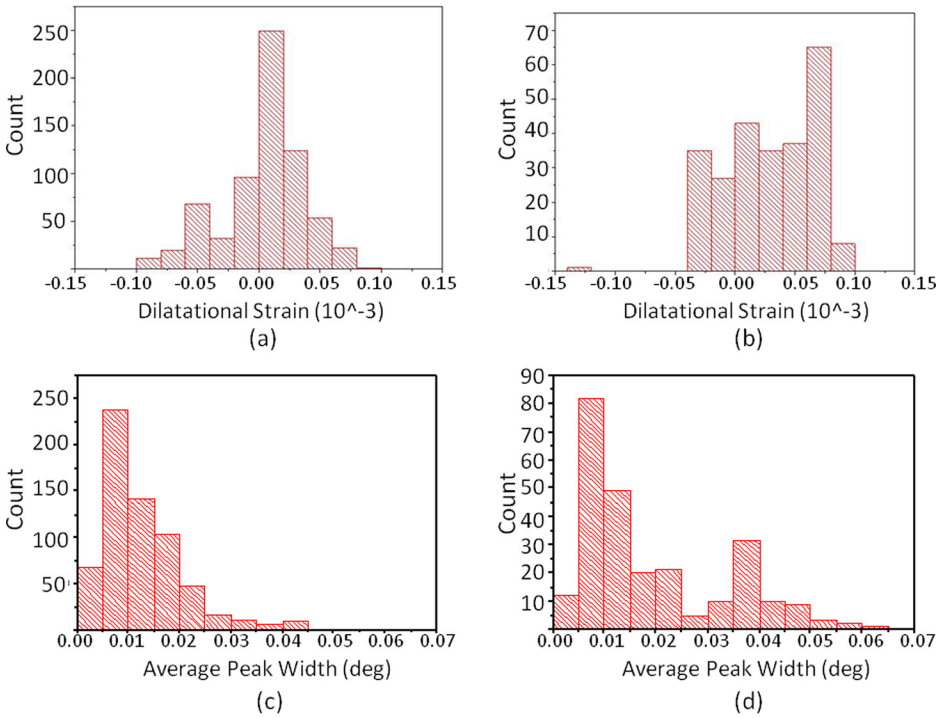

FIG. 1. Dilatation strain for (a) untreated particles and (b) particles annealed to 573 K. Counts represent number of pixels in the map where particles are present rather than number of particles. Average diffraction peak width for (c) untreated particles and (d) particles annealed to 573 K.

characterizes heterogeneity of stresses within a particle. Heat treatment causes significant increase in the magnitude of stress heterogeneity. This heterogeneity is usually caused by heterogeneity in crystal orientations and consequently distribution of the elastic moduli tensor in polycrystalline Al particles. According to linear elasticity theory, the stress heterogeneity should be proportional to the applied or average stress, i.e., to the mean stress σ_0 due to different thermal contraction from T_0 to room temperature. Thus, Figs. 1(a), 1(b) and 1(c), 1(d) are qualitatively consistent.

Let us compare these results with theoretical estimates based on equations for mean stress in the Al core and maximum tensile hoop stress in the Al_2O_3 shell at the interface with the Al core, σ_h (see Refs. 6 and 8)

$$\sigma_0 = \frac{12(m^3-1)\left(\varepsilon_2^T-\varepsilon_1^T\right)G_2K_1K_2}{H} - \frac{2K_1(4G_2+3m^3K_2)\Gamma_1}{RH} - \frac{2\Gamma_2 m^2K_1(4G_2+3K_2)}{RH}, \tag{1}$$

$$\sigma_h = -\frac{6(m^3+2)\left(\varepsilon_2^T-\varepsilon_1^T\right)G_2K_1K_2}{H} - \frac{4(m^3+2)G_2K_2\Gamma_1}{RH} - \frac{2\Gamma_2 m^2(-2G_2K_1+3(2G_2+K_1)K_2)}{RH}, \tag{2}$$

$$\varepsilon_1^T = \alpha_1(T-T_0), \quad \varepsilon_2^T = \alpha_2(T-T_0),$$
$$H = 3m^3K_1K_2 + 4G_2(K_1+(m^3-1)K_2). \tag{3}$$

Here, subscripts 1 and 2 designate Al and Al_2O_3, respectively, $m = 1 + 1/M$, G and K are the shear and bulk moduli, $\Gamma_1 = \Gamma_2$ are the surface stresses (in Refs. 6 and 8 these parameters are designated as surface energies) at the core-shell and shell-gas interfaces, α is the linear thermal expansion coefficient, and T is the particle temperature at the instant of strain measurement, i.e., room temperature. Since we will consider large M, from 500 to 2000, Eqs. (1) and (2) can be simplified by using a Taylor series expansion for small value $m - 1 = 1/M$ and keeping just the linear terms

$$\sigma_0 = \frac{36\left(\varepsilon_2^T-\varepsilon_1^T\right)G_2K_1K_2}{MH_s} - \frac{4\Gamma}{RH_s}, \quad H_s = (3K_2+4G_2)K_1, \tag{4}$$

$$\sigma_h = -\frac{18\left(\varepsilon_2^T-\varepsilon_1^T\right)G_2K_1K_2}{H_s} - \frac{12G_2K_2\Gamma}{RH_s} - \frac{2\Gamma(-2G_2K_1+3(2G_2+K_1)K_2)}{RH_s}. \tag{5}$$

Material properties are given in Table I. They differ from those in Ref. 6 because in Ref. 6 they were defined at Al melting temperature and here at room temperature. Substituting these properties in Eqs. (4) and (5), we obtain

$$\sigma_0(\text{MPa}) = \frac{18.7573(T_0-T)}{M} - \frac{4\Gamma}{R},$$
$$\sigma_h(\text{MPa}) = 9.3786(T-T_0) - \frac{9.823\Gamma}{R}. \tag{6}$$

Similar to Refs. 15 and 16, we consider that for untreated particles $T_0 = T_r$, i.e., T_0 is equal to the room temperature. For $T_0 = T$ (i.e., for untreated particles at room temperature), the first terms in Eq. (6) disappear and the contribution due to surface stress remains only. Experimental measurements gave positive $\sigma_0 = 0.296$ MPa for this case, which is possible for negative Γ only. While for liquid-liquid interface surface

TABLE I. Material parameters for aluminum (subscript 1) and alumina (subscript 2) at room temperature.

K_1 (GPa)[21]	K_2 (GPa)[22]	G_2 (GPa)[22]	$\alpha_1(10^5\,K^{-1})$[21]	α_2 $(10^5\,K^{-1})$[22]
76	252	163	2.33	0.54

stress is equal to surface energy and is positive, for interfaces involving solids this is not the case and there is nothing that excludes negative interface stresses.[23–25] Also, there may be other sources of internal stresses besides thermal strain and surface stresses, e.g., internal stresses due to defects (grain boundaries, dislocations, and point defects). We can add stresses due to these sources or effectively include all of them in Γ, and from condition $-\frac{4\Gamma}{R} = 0.296$ MPa will find $\Gamma = -0.074\ R$. For a typical particle size: R = 2000 nm, Γ = −148 MPa nm = −0.148 GPa nm. This magnitude is 7 times smaller than the assumed interface energy of 1.05 GPa nm.[6] Substituting Γ/R in Eq. (6), we further simplify

$$\sigma_0(MPa) = \frac{0.0187573(T_0 - T)}{M} + 0.296,$$
$$\sigma_h(MPA) = 9.3786(T - T_0) + 0.727. \quad (7)$$

Plot of σ_0 versus M for $T_0 = 473$ K and $T = 298$ K is shown in Fig. 2. In the entire range of M, values of σ_0 are an order of magnitude larger than the contribution 0.296 MPa due to surface stresses and other unknown sources. Thus, these uncertainties are not important. More importantly is that the range of σ_0 in Fig. 1, from 2 to 7 MPa, overlaps with the range of experimental values that was discussed above. Thus, in experiments, the maximum volume of Al exhibits mean stresses from 4.56 to 6.08 MPa, which corresponds to M from 568 to 770 in Eq. (7). If we take $\delta = 3$ nm (see Fig. 3 in Ref. 16), these M correspond to R from 1.704 to 2.310 μm, which are reasonable numbers for particles with a size distribution shown in Fig. 4 in Ref. 16. Averaged over the volume experimental stress $\sigma_0 = 2.18$ MPa corresponds to M = 1742, which for $\delta = 3$ nm gives R = 5.226 μm. While there may be just few such particles in the study, they produce the major contribution to the volume distribution of the particle size (see Figure 4(b) in Ref. 16). Note that contribution to the flame speed according to MDM is also proportional to the total volume of melt, which led to the fracture of oxide shell during fast heating, normalized by the total volume of particles. Thus, results of experiments and theoretical predictions on the mean stress that appears after annealing are in very good agreement, which is not affected by existing indeterminacies in additional sources of internal stresses and particles geometric parameters.

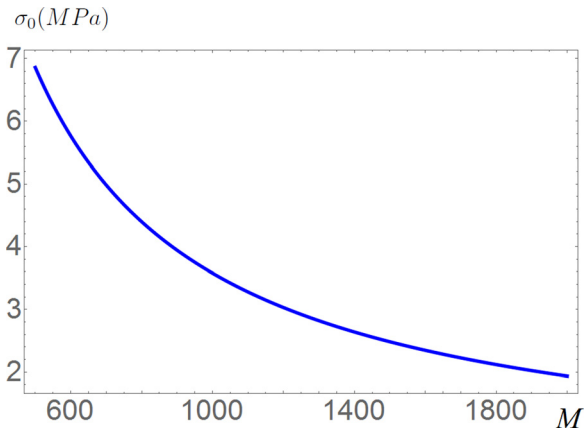

FIG. 2. Theoretical dependence of the tensile mean stress σ_0 in Al core after treatment annealing and fast heating at $T_0 = 473$ K on $M = R/\delta$ according to Eq. (7).

Despite the small level of the mean tensile stress in Al, the main effect is in producing large compressive stresses in alumina that will delay fracture of the oxide shell during fast heating in the flame.[6,15,16] Substituting $T_0 = 473$ K and $T = 298$ K in Eq. (7), we obtain $\sigma_h = 1.641$ GPa. This is quite high stress, which is 14% of the estimated theoretical strength for alumina shell. Hoop stress is independent of M, i.e., despite the broad distribution of M and consequently σ_0, hoop stress is fixed by the value of $T_0 - T$. Surface stresses are negligible in Eq. (7).

IV. CONCLUDING REMARKS

The measurements of mean stresses in Al micron scale particles covered by and Al_2O_3 shell are performed using x-ray diffraction with synchrotron radiation. Both untreated and heat treated (i.e., annealed at elevated temperature) particles have been studied. Also, flame speed for the mixture of these particles and CuO oxidizer has been measured. For Al particles annealed at 573 K and quenched with high cooling rate, flame rate increased by 32% in comparison with untreated particles. This improvement is consistent with experiments and MDM-based theory[16] for the temperature $T_0 = 473$ K, at which particles are stress-free. This means that increasing annealing temperature above 473 K does not further improve reactivity for given flame propagation experiments. This may be related to the fact that at cooling from such a high temperature internal stresses have time to partially relax and are approximately at the same level as at annealing at 473 K. For this reason, $T_0 = 473$ K is used in the theoretical estimates. Measured tensile stress in the Al core is in the range from 2 to 7 MPa, and in very good agreement with experiments for M from 0.568 to 2.310 μm. These are reasonable M values for particles with a size distribution shown in Fig. 4 in Ref. 16. Such a relatively small stress in Al core causes a large compressive hoop stress in the Al_2O_3 shell, $\sigma_h = 1.641$ GPa. The hoop stress is independent of M and surface stresses and it delays fracture of the oxide shell during fast heating in the flame.[6,15,16] Thus, obtained results confirm that the reason of improvement of Al reactivity of Al particles in the flame is related to their pre-stressing, according to MDM. Since compressive stresses in the shell suppress diffusion, this improvement is in contradiction with traditional diffusion reaction mechanism through the alumina shell.

Note that reduction in M increases mean stress proportionally (Eq. (7)), which may enable us to perform stress measurements even with the less precise techniques. This can be done either by reducing particle size or by growing thicker shells. Also, our main goal is to quantify hoop stresses in the shell rather than in the core. This can be done if preliminary to transform shell from amorphous to crystalline. According to Ref. 26, this does not affect flame speed.

Obtained results represent an important step in our main goal in designing Al particles for energetic applications. Instead of reducing particle size to the nanoscale, we suggest

to utilize few micrometer size pre-stressed particles. They exhibit almost the same reactivity as the best nanoparticles, but are 30–50 times less expensive and do not possess safety and environmental issues.

ACKNOWLEDGMENTS

The authors are grateful for support from ONR under contract managed by Dr. C. Bedford. The Advanced Light Source was supported by the Director, Office of Science, Office of Basic Energy Sciences, Materials Sciences Division, of the U.S. Department of Energy under Contract No. DE-AC02-05CH11231 at Lawrence Berkeley National Laboratory and University of California, Berkeley, California.

[1]B. S. Bockmon, M. L. Pantoya, S. F. Son, B. W. Asay, and J. T. Mang, J. Appl. Phys. **98**, 064903 (2005).
[2]V. E. Sanders, B. W. Asay, T. J. Foley, B. C. Tappan, A. N. Pacheco, and S. F. Son, J. Propul. Power **23**, 707 (2007).
[3]J. Y. Malchi, R. A. Yetter, S. F. Son, and G. A. Risha, Proc. Combust. Inst. **31**, 2617 (2007).
[4]V. I. Levitas, M. L. Pantoya, and B. Dikici, Appl. Phys. Lett. **92**, 011921 (2008).
[5]C. D. Yarrington, S. F. Son, T. J. Foley, S. J. Obrey, and A. N. Pacheco, Propellants, Explos., Pyrotech. **36**, 551 (2011).
[6]V. I. Levitas, B. W. Asay, S. F. Son, and M. Pantoya, J. Appl. Phys. **101**, 083524 (2007).
[7]V. I. Levitas, Combust. Flame **156**, 543 (2009).
[8]V. I. Levitas, Philos. Trans. R. Soc. A **371**, 20120215 (2013).
[9]V. Rosenband, Combust. Flame **137**, 366 (2004).
[10]S. Chowdhury, K. Sullivan, N. Piekiel, L. Zhou, and M. R. Zachariah, J. Phys. Chem. C **114**, 9191 (2010).
[11]D. A. Firmansyah, K. Sullivan, K. S. Lee, Y. H. Kim, R. Zahaf, M. R. Zachariah, and D. Lee, J. Phys. Chem. C **116**, 404 (2012).
[12]Y. Ohkura, P. M. Rao, and X. Zheng, Combust. Flame **158**, 2544 (2011).
[13]V. I. Levitas, M. L. Pantoya, and K. W. Watson, Appl. Phys. Lett. **92**, 201917 (2008).
[14]V. I. Levitas, M. L. Pantoya, and S. Dean, Combust. Flame **161**, 1668 (2014).
[15]V. I. Levitas, B. Dikici, and M. L. Pantoya, Combust. Flame **158**, 1413 (2011).
[16]V. I. Levitas, J. McCollum, and M. L. Pantoya, Sci. Rep. **5**, 7879 (2015).
[17]Q. S. Mei, S. C. Wang, H. T. Cong, Z. H. Jin, and K. Lu, Acta Mater. **53**, 1059 (2005).
[18]B. Rufino, M.-V. Coulet, R. Bouchet, O. Isnard, and R. Denoyel, Acta Mater. **58**, 4224 (2010).
[19]N. Tamura, "XMAS: A versatile tool for analyzing synchrotron x-ray microdiffraction data," *Microdiffraction Analysis of Local and Near Surface Hierarchical Organization of Defects* (Imperial College Press, London, UK, 2013).
[20]M. Kunz, N. Tamura, K. Chen, A. A. MacDowell, R. S. Celestre, M. M. Church, and E. Ustundag, Rev. Sci. Instrum. **80**, 035108 (2009).
[21]S. Raju, K. Sivasubramanian, and E. Mohandas, Solid State Commun. **122**, 671 (2002).
[22]O. L. Anderson, *Equations of State of Solids for Geophysics and Ceramic Science* (Oxford University Press, Oxford, UK, 1995), p. 362.
[23]F. D. Fischer, T. Waitz, D. Vollath, and N. K. Simha, Prog. Mater. Sci. **53**, 481 (2008).
[24]V. I. Levitas and K. Samani, Nat. Commun. **2**, 284 (2011).
[25]V. I. Levitas and K. Samani, Phys. Rev. B: Rapid Commun. **84**, 140103(R) (2011).
[26]V. I. Levitas, M. L. Pantoya, G. Chauhan, and I. Rivero, J. Phys. Chem. C **113**, 14088 (2009).